https://doi.org/10.5194/egusphere-2024-736
Preprint. Discussion started: 22 March 2024

Characterizing water solubility of fresh and aged secondary organic aerosol in $PM_{2.5}$ with the stable carbon isotope technique

Fenghua Wei[1], Xing Peng[1], Liming Cao[1], Mengxue Tang[1], Ning Feng[1], Xiaofeng Huang[1], Lingyan He[1]

[1]Laboratory of Atmospheric Observation Supersite, School of Environment and Energy, Peking University Shenzhen Graduate School, Shenzhen 518055, China.

Correspondence: Xing Peng (pengxing@pku.edu.cn)

https://doi.org/10.5194/egusphere-2024-736
Preprint. Discussion started: 22 March 2024

Abstract: The investigation of the water-soluble characteristics of secondary organic carbon (SOC) is essential for a more comprehensive understanding of its climate effects. However, due to the limitations of the existing source apportionment methods, the water solubility of different types of SOC remains uncertain. This study analyzed stable carbon isotope and mass spectra signatures of total carbon (TC) and water-soluble organic carbon (WSOC) in ambient $PM_{2.5}$ samples for one year and established stable carbon isotope profiles of fresh and aged SOC. Furthermore, the Bayesian stable isotope mixing (BSIM) model was employed to reveal the water solubility characteristics of fresh and aged SOC in a coastal megacity of China. WSOC was dominated by secondary sources, with fresh and aged SOC contributing 28.1 % and 45.2 %, respectively. Water-insoluble organic carbon (WIOC) was dominated by primary sources, to which fresh and aged SOC contributed 23.2 % and 13.4 %. We also found the aging degree of SOC has considerable impacts on its water solubility due to the much higher water-soluble fraction of aged SOC (76.5 %) than fresh SOC (54.2 %). Findings of this study may provide a new perspective for further investigation of the hygroscopicity effects of SOC with different aging degrees on light extinction and climate change.

Keywords: Fresh SOC; Aged SOC; Water solubility; Stable carbon isotope; BSIM model; Mass spectrometry.

Graphical abstract:

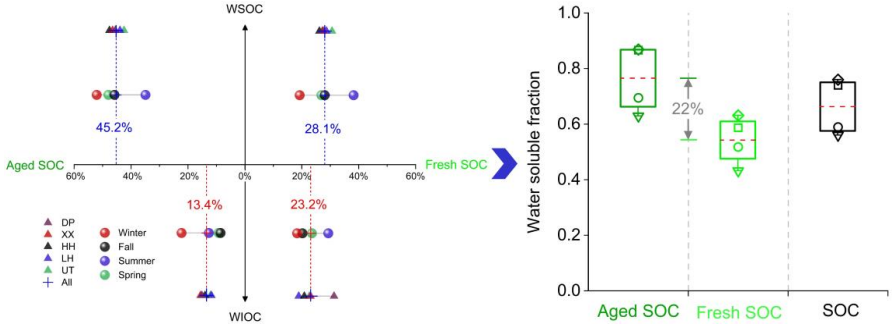

https://doi.org/10.5194/egusphere-2024-736
Preprint. Discussion started: 22 March 2024

1. Introduction

As a major component of particulate matter ($PM_{2.5}$), secondary organic aerosols (SOA) not only contribute to haze formation but also exert a substantial influence on climate dynamics across various spatial scales, from local to global (Kaul et al., 2011; Shrivastava et al., 2017). The water solubility, considered one of the crucial physical properties of SOA, has been extensively studied recently due to its significant effects on the physicochemical processes in the atmosphere. The water solubility of SOA varied with its aging degrees (Kirillova et al., 2013), while both the water solubility and aging degree of organic aerosols contribute to the hygroscopicity noticeably, which affects the light extinction eventually (Han et al., 2022; Liu et al., 2022). Hence, exploring the water solubility characteristics of SOA with different aging degrees can help elucidate the more detailed extinction mechanism of SOA. In addition, recent studies have also shown that the formation of secondary particulates is one of the main processes determining the amount of CCN in remote oceanic regions (Liu and Matsui 2022). Therefore, investigating the water solubility of SOA with different aging degrees is also meaningful for further exploring its indirect climate effects.

Investigating the contributions of SOA with different aging degrees to both organic matter (OM) and water-soluble organic matter (WSOM) is imperative for determining their quantified water solubility. However, due to the constraints of reliable methods, only a limited number of studies have examined the water solubility of SOA using mass spectrometry techniques. Qiu et al. (2019) conducted source apportionment of OM in PM_1 and WSOM in $PM_{2.5}$ based on online and offline AMS-PMF methods respectively (Qiu et al., 2019). This approach faces challenges not only related to the inherent errors of online versus offline methods but also discrepancies in the measured particle sizes of OM and WSOM. Kondo et al. (2007) and Timonen et al. (2013) attempted to apportion water-soluble organic carbon

https://doi.org/10.5194/egusphere-2024-736
Preprint. Discussion started: 22 March 2024

(WSOC) through a multiple linear regression method based on the mass spectral information of OM, which still exhibits large indeterminateness (Timonen et al., 2013; Xiao et al., 2011; Kondo et al., 2007). The carbon isotopic technique offers a promising avenue to overcome the aforementioned limitations, thereby enabling a more in-depth exploration of the water-soluble characteristics of SOA. Carbon isotope techniques have garnered widespread attention and are increasingly employed in source apportionment studies of organic aerosols due to their robust source appointment capabilities. Radioactive carbon isotopes (^{14}C) provide a precise method for quantitatively distinguishing between fossil and non-fossil organic aerosol sources (Fushimi et al., 2011; Zhang et al., 2014). The stable carbon isotope technique (^{13}C), however, can quantitatively assess the contributions of various sources by integrating them into mass balance models (Yao et al., 2022; Widory et al., 2004). The Bayesian mixing model stands out as one of the most widely utilized models (Xiao;Xu and Xiao 2023; Tang et al., 2020). The stable carbon isotope technique can also be combined with other source tracers to further enhance the accuracy of source apportionment of carbonaceous aerosols (Jiang et al., 2022; Plasencia Sánchez et al., 2023; Ceburnis et al., 2011; Lim et al., 2022). However, to our knowledge, no study has employed the carbon isotope technique to estimate the source contribution of both fresh and aged SOA before, owing to the challenging measurement of the carbon isotope profiles for these two sources.

Previous studies have predominantly concentrated on assessing the water solubility of SOA at inland urban sites, revealing a strong correlation between SOA water solubility and urban air pollution emissions as well as relative humidity (Wong;Zhou and Abbatt 2015; Pye et al., 2017; Favez et al., 2008; Salma et al., 2007; Weber et al., 2007; Miyazaki et al., 2006). Nevertheless, few researchers have noticed the differences between inland and coastal cities. As dynamic interfaces between urban and marine environments (Donaldson and George 2012), coastal cities exhibit unique characteristics. Shenzhen is a

https://doi.org/10.5194/egusphere-2024-736
Preprint. Discussion started: 22 March 2024

typical representative city for coastal air pollution studies with a coastline spanning 260.5 km and a total sea area of 1145 m^2. We measured the stable carbon isotope end-members of fresh and aged secondary organic carbon (SOC), which enables us to investigate the source contributions of SOC with different aging degrees to WSOC and their respective water solubility in Shenzhen.

The aim of this study is to investigate the water solubility of SOC in $PM_{2.5}$, emphasizing Shenzhen as a representative mega-coastal city in China. We analyzed stable carbon isotopes and mass spectra signatures of total carbon (TC) and WSOC in ambient $PM_{2.5}$ samples that were collected from five distinct sites in Shenzhen over one year as well as specific emission sources. For the first time, we employed the Bayesian stable isotope mixing (BSIM) model on localized source profiles to quantify the contributions of fresh SOC and aged SOC to WSOC and water-insoluble organic carbon (WIOC). These results would contribute to estimating the water solubility of both fresh and aged SOC, revealing their direct or indirect implications for climate change.

2. Material and methods

2.1 Ambient $PM_{2.5}$ sampling and chemical analysis

Shenzhen (N22°27′ ~ N22°52′, E113°46′ ~ E114°37′), one megacity of Pearl River Delta, China, is bordered by Daya Bay and Dapeng Bay to the east, the Pearl River Estuary and Lingding Sea to the west, Hong Kong to the south, and Dongguan and Huizhou to the north. As a typical mega-coastal city in China, Shenzhen's air quality is predominantly affected by the continental air mass from northern Guangdong, the eastern coastal air mass, and the southern marine air mass (Fig. 1). For a comprehensive exploration of pollution characteristics in Shenzhen, $PM_{2.5}$ samples were collected from five sites covering the western to eastern regions of the city. The selected sites are Xixiang (XX, urban site), University Town

https://doi.org/10.5194/egusphere-2024-736
Preprint. Discussion started: 22 March 2024

(UT, urban site), Longhua (LH, urban site), Honghu (HH, urban site), and Dapeng (DP, background site) (Fig. 1). Additional details about each sampling site are listed in Table S1.

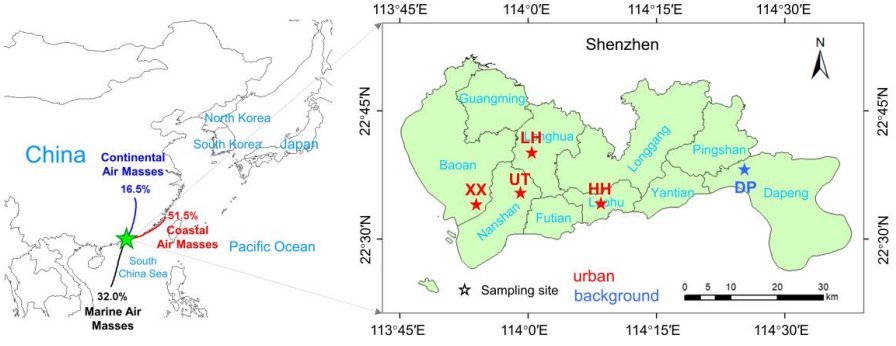

Figure 1. Spatial distribution of the five sampling sites in Shenzhen for this study.

In this study, 24-hour $PM_{2.5}$ sampling was conducted every other day in 2019 at the UT site using a Thermo 2300 atmospheric particulate sampler (Thermo Fisher Scientific Inc., Waltham, Massachusetts, USA), yielding a total of 160 valid samples. For the remaining four sites, a total of 295 valid $PM_{2.5}$ samples were collected every other day during typical months of the four seasons in 2019 (March, June, September, and December, Table S2) using a Model TH-16A atmospheric particulate sampler (Tianhong Corp., Wuhan, China). The organic carbon (OC) and elemental carbon (EC) in $PM_{2.5}$ were analyzed using an OC/EC analyzer (2001A, Desert Research Institute, Reno, Nevada, USA) following the IMPROVE A procedure.

For WSOC extraction, the $PM_{2.5}$ sample underwent ultrasonication (20 min × 3 times) in 15 ml ultrapure water (18.2 MΩ·cm), followed by filtration through a syringe with a 0.45 μm filter head to eliminate insoluble particles. The extracted $PM_{2.5}$ samples were sequentially analyzed using a long-time-of-flight aerosol mass spectrometer (L-TOF-AMS, Aerodyne, USA) and an ultrasonic nebulizer (U5000AT+, Cetac Technologies Inc., USA) to measure elemental ratios, such as O/C, as well as the

https://doi.org/10.5194/egusphere-2024-736
Preprint. Discussion started: 22 March 2024

mass spectrum signatures of the water-soluble organic fractions, including ion fragments like CO_2^+, $C_4H_9^+$, and $C_2H_4O_2^+$. The concentration of WSOC was determined using a total organic carbon analyzer (multi N/C 3100, Jena, Germany), and WIOC was calculated as the difference between OC and WSOC.

To investigate the stable carbon isotope signatures of carbonaceous aerosols, we built a stable isotope spectrometry system by integrating an OC/EC analyzer with a carbon dioxide isotope spectrometer (QCLAS, Aerodyne). This system reduces the carbon requirement for isotope analysis from 5 μgC to 0.5 μgC and improves the accuracy of spectroscopic measurement methods to 0.2‰~0.3‰. The stable carbon isotope values of TC and WSOC in ambient $PM_{2.5}$ were measured in this study.

2.2 Bayesian stable isotope mixing model

The BSIM model could quantify the contributions of multiple sources to the TC and WSOC based on the principle of mass conservation of stable isotopes, in which the Markov Chain Monte Carlo (MCMC) method was employed. The methodology employed in the BSIM model was detailed in works by Parnell et al. (2013) and Parnell and Inger (2010) (Parnell et al., 2010; Parnell et al., 2013). In brief, the posterior distribution for the Bayesian neural network (BNN) was calculated utilizing the prior distribution and likelihood function based on Bayes theorem. Implementation of the BSIM model in this study utilized the SIMMR package in R software (https://cran.r-project.org/ web/packages/simmr/index.html). Gelman diagnostic values, ranging from 1 to 1.01, all met the criteria of the posterior prediction test, indicating robust model performance and reliable results. Additionally, an uncertainty index (UI_{90}) was employed here to further characterize the uncertainty strength of TC and WSOC source apportionments based on their posterior distribution. This index refers to the difference between the proportional contributions of the maximum and minimum values in the rapid increase segment divided by 90 with a 90 % cumulative probability ($UI_{90} = (PC_{95}\text{-}PC_5)/90$) (Zaryab et al., 2022; Ji et al., 2017).

https://doi.org/10.5194/egusphere-2024-736
Preprint. Discussion started: 22 March 2024

2.3 Stable carbon isotope spectrum of $PM_{2.5}$ sources

The BSIM model requires the input of potential sources for carbonaceous aerosols, along with their local source-specific stable carbon isotope values (end-members). The PMF model was employed to identify the TC sources based on $PM_{2.5}$ chemical species concentrations (carbon components, water-soluble inorganic ions, elements, Text S1), and found traffic sources, secondary transformation sources, and biomass combustion sources as the major contributors to carbonaceous aerosols in Shenzhen, which are similar to the previous results in Guangzhou (Huang et al., 2014). Secondary conversion sources could be further subdivided into fresh SOC for the low oxidation state and aged SOC for the high oxidation state (Chen et al., 2019; Presto et al., 2009; Mahrt et al., 2022; Shen et al., 2017). Ultimately, traffic emissions, fresh SOC, aged SOC, and biomass burning (BB) were identified as the four potential sources of TC and WSOC in Shenzhen in this study.

Recognizing the regional variability in stable carbon isotope fingerprints of $PM_{2.5}$ sources (Yao et al., 2022), this work obtained representative and locally specific carbon isotope profiles for the four sources in Shenzhen. For the traffic emissions, we measured the stable carbon isotope values of TC and WSOC in $PM_{2.5}$ that were collected from the Mount Tanglang tunnel (dominated by diesel vehicles) and the Jiuweiling tunnel (dominated by petrol vehicles) in Shenzhen. Fresh SOC was simulated through petrol vehicle bench tests, and the oxygen-carbon ratio (O/C) of $PM_{2.5}$ samples ranges from 0.51 to 0.62, indicating a low oxidation state of SOA (Ding et al., 2012). The lowest stable carbon isotope values for TC and WSOC from the simulated sample were chosen as the fresh SOC results. Aged SOC samples were obtained by collecting ambient $PM_{2.5}$ samples at the National Ambient Air Background Monitoring Station (Mount Wuzhi site, Hainan, China), primarily influenced by regional pollution transported by northern continental air masses. These ambient $PM_{2.5}$ samples exhibited a high O/C value of 0.98,

https://doi.org/10.5194/egusphere-2024-736
Preprint. Discussion started: 22 March 2024

suggesting their highly oxidized state (Zhu et al., 2016). Biomass burning emissions were simulated and analyzed by burning pine wood in the Laboratory of Biomass Burning Simulation at Peking University Shenzhen Graduate School (He et al., 2010). Additional details about the sampling process are available in the Supplementary Information (Text S2). Table 1 summarizes the stable carbon isotope values of the four sources used in this study. Table S3 compares $\delta^{13}C_{TC}$ source signatures in this study with global datasets, indicating that the measurement results fall within the range of global datasets. Previous research identified $C_2H_4O_2^+$ (*m/z 60*) as a reliable marker for biomass burning in Shenzhen, with a feature value of 1.61±0.68 % (Cao et al., 2018). This prior information was also incorporated into the BSIM model to estimate the biomass burning source.

Table 1. Stable carbon isotope end-members and f_{60} signatures for TC and WSOC sources.

	Traffic		Fresh SOC		Aged SOC		BB	
TC	$\delta^{13}C$/‰	f_{60}/%	$\delta^{13}C$/‰	f_{60}/%	$\delta^{13}C$/‰	f_{60}/%	$\delta^{13}C$/‰	f_{60}/%
	-26.26±0.50	0	-27.31±0.73	0	-25.54±0.28	0	-27.58±0.24	1.61±0.68
	Traffic		Fresh SOC		Aged SOC		BB	
WSOC	$\delta^{13}C$/‰	f_{60}/%	$\delta^{13}C$/‰	f_{60}/%	$\delta^{13}C$/‰	f_{60}/%	$\delta^{13}C$/‰	f_{60}/%
	-26.68±0.37	0	-26.18±0.75	0	-24.93±0.39	0	-26.78±0.17	1.61±0.68

2.4 Contributions of SOC to WIOC

Based on the source apportionment results from the BISM model for TC and WSOC, the contributions of fresh SOC and aged SOC to WIOC were calculated according to the equations (1-2). The uncertainties (u) in concentrations of Fresh SOC $_{(WIOC)}$ and Aged SOC $_{(WIOC)}$ were assessed using the uncertainty transfer equations (3-4). Fresh SOC and aged SOC uncertainties in both TC (14.9 %, 30.1 %) and WSOC (24.1 %, 20.9 %) were determined using the BSIM model. Our findings reveal that the calculated uncertainties of [Fresh SOC $_{(WIOC)}$] and [Aged SOC $_{(WIOC)}$] were 28.3 % and 36.8 %, respectively.

$$[\text{Fresh SOC}_{(WIOC)}] = [\text{Fresh SOC}_{(TC)}] - [\text{Fresh SOC}_{(WSOC)}] \quad (1)$$

https://doi.org/10.5194/egusphere-2024-736
Preprint. Discussion started: 22 March 2024

$$[\text{Aged SOC}_{(\text{WIOC})}] = [\text{Aged SOC}_{(\text{TC})}] - [\text{Aged SOC}_{(\text{WIOC})}] \quad (2)$$

$$u_{[\text{Fresh SOC}_{(\text{WIOC})}]} = \left(u^2_{[\text{Fresh SOC}_{(\text{TC})}]} + u^2_{[\text{Fresh SOC}_{(\text{WSOC})}]}\right)^{1/2} \quad (3)$$

$$u_{[\text{Aged SOC}_{(\text{WIOC})}]} = \left(u^2_{[\text{Aged SOC}_{(\text{TC})}]} + u^2_{[\text{Aged SOC}_{(\text{WSOC})}]}\right)^{1/2} \quad (4)$$

3. Results and discussion

3.1 Overview of $PM_{2.5}$ and carbonaceous components

The annual mean concentration of $PM_{2.5}$ in Shenzhen was 24.9 μg/m^3 in 2019, with TC being the predominant component, exhibiting an annual mean concentration of 7.1 μg/m^3 (5.8 and 1.3 μg/m^3 for OC and EC, respectively). WSOC accounts for 48 % of OC, presenting an annual mean concentration of 2.8 μg/m^3. The mean stable carbon isotope values for TC ($\delta^{13}C_{TC}$) and WSOC ($\delta^{13}C_{WSOC}$) were -26.64 ± 0.79 ‰ and -25.80 ± 0.88 ‰, respectively, which is lower than the results of northern cities in China (Wu et al., 2020). This can be attributed to the limited impact of coal combustion (which has high ^{13}C values) on $PM_{2.5}$ in Shenzhen (Yao et al., 2022; Vodicka et al., 2022).

Seasonal variation revealed that TC, OC, WSOC, and EC exhibited elevated levels in winter and decreased levels in summer (Fig. 2a). This pattern primarily stems from pollution air masses originating from continental regions in the fall and winter, and clean air masses from the southern ocean during the summer months (Fig. S1). The OC to EC ratio, averaging 4.5, was also higher in winter than in summer, consistent with the Oxygen-to-Carbon (O/C) ratio results for WSOC (Fig. 2a), indicating a large influence of aged SOC on carbonaceous aerosols in winter. The stable carbon isotope results support this observation. Figure 2b depicts relatively higher $\delta^{13}C_{TC}$ and $\delta^{13}C_{WSOC}$ values in spring (-26.59‰, -25.26‰), fall (-26.38‰, -25.44‰), and winter (-26.46‰, -26.27‰). These higher values are attributed to greater contributions of aged SOC from northern and northeast regional transport processes during

https://doi.org/10.5194/egusphere-2024-736
Preprint. Discussion started: 22 March 2024

these seasons (Fig. S1). In summer, observed low $\delta^{13}C_{TC}$ and $\delta^{13}C_{WSOC}$ values of -27.29‰ and -26.57‰, respectively, suggest relatively high contributions of fresh SOC to $PM_{2.5}$. Shenzhen experiences high temperatures in summer, leading to increased gaseous precursor emissions from terrestrial biogenic sources, especially C3 plants. Intense solar radiation and high temperature favor photochemical reactions to generate fresh SOC that depletes ^{13}C in particulate matter during summer (Kirillova et al., 2013).

Mass spectra characteristics of CO_2^+ (*m/z 44*), $C_4H_9^+$ (*m/z 57*), and $C_2H_4O_2^+$ (*m/z 60*) in WSOC were measured to represent oxidized organic aerosol (OOA), hydrocarbon-like organic Aerosol (HOA), and biomass burning organic aerosol (BBOA), respectively. The abundance of these ion fragments, denoted as f_{44}, f_{57}, and f_{60}, is determined by the ratios of signal intensities at *m/z 44*, *m/z 57*, and *m/z 60* to the sum of signal intensities from all *m/z* signals in the organic mass spectra. As depicted in Fig. 2c, f_{44} obtained higher values in spring (0.131) and winter (0.125) compared to summer (0.120) and fall (0.112), further indicating an elevated oxidation level of OOA during spring and winter. Considering that f_{60} exceeds 0.0030 when biomass burning influences carbonaceous aerosol (Docherty et al., 2008; DeCarlo et al., 2008), the annual average value of f_{60} was 0.0032, suggesting biomass burning was an important source of carbon components in Shenzhen. Winter exhibited higher levels of f_{60} (0.0035) compared to other seasons, suggesting relatively strong impacts of biomass burning on WSOC in winter. Conversely, f_{57} reached its highest level in summer (0.014) and the lowest in winter (0.009), with an annual average value of 0.011, possibly associated with a notable increase in hydrocarbon organic aerosol emissions from traffic and biogenic sources during the summer period.

https://doi.org/10.5194/egusphere-2024-736
Preprint. Discussion started: 22 March 2024

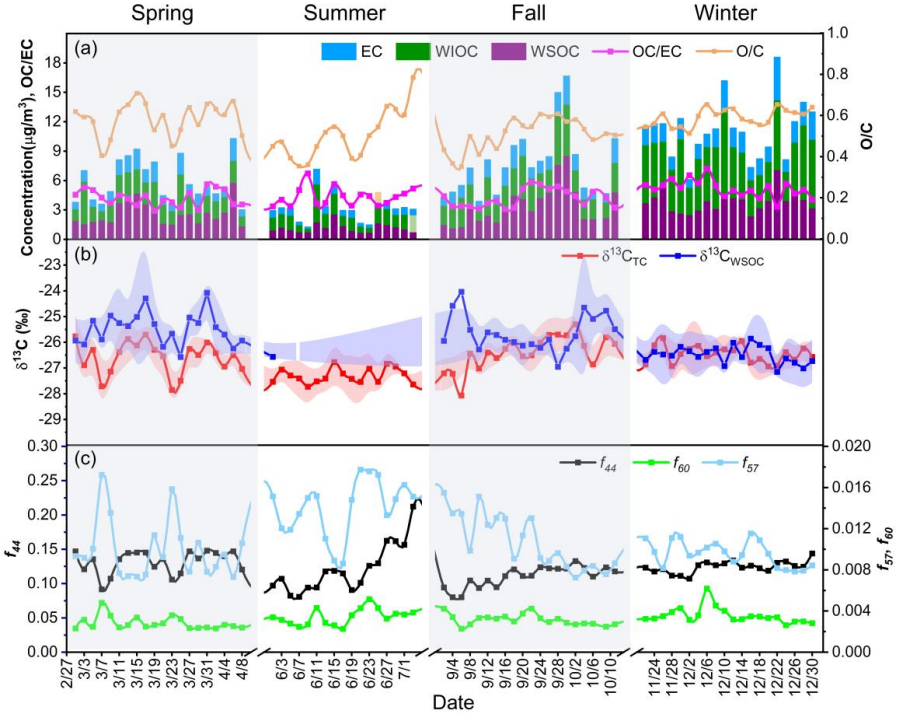

Figure 2. Time series of carbonaceous components (a), stable carbon isotope characteristics of TC and WSOC(b), and mass spectra signatures of WSOC in $PM_{2.5}$ (c) from Shenzhen. Each data was averaged from five sampling sites. (Note: Summer samples exhibit elevated analytical errors due to low concentrations, and $\delta^{13}C_{WSOC}$ values are computed from combined summer samples).

Obvious spatial variations in $PM_{2.5}$ mass concentrations across Shenzhen during 2019 were observed, with XX site registering the highest concentration (29.6 μg/m^3), followed by LH (28.0 μg/m^3), HH (23.4 μg/m^3), UT (23.1 μg/m^3), and DP (20.2 μg/m^3). Figure 3 illustrates that TC made more substantial contributions (28.2 %~32.5 %) to $PM_{2.5}$ at the four urban sites in the central and western regions of Shenzhen compared to the background site (DP, 25.7 %). This suggests that local pollutant emissions significantly influence carbonaceous aerosols in Shenzhen's urban areas. The percentage of WSOC in TC was also higher in urban areas (37.5±3.9 %) compared to the background area (DP, 33.2 %),

https://doi.org/10.5194/egusphere-2024-736
Preprint. Discussion started: 22 March 2024

reaching the highest value at the LH site (42.9 %). However, the percentage of WIOC in TC displayed the opposite trend, suggesting carbonaceous aerosols in urban areas of Shenzhen exhibit higher water solubility than in background areas. Distinct spatial distribution characteristics were also observed in the stable carbon isotopes of TC and WSOC. The background site exhibits higher $\delta^{13}C_{TC}$ values (-26.33 %) than the four urban sites (-26.72±0.13 %). This difference may be attributed to the increased contribution of traffic or fresh SOC sources to carbonaceous aerosols at urban sites and the relatively high contribution of aged SOC at the background site. Atmospheric aging processes of organics through photochemical reactions can deplete ^{13}C in aged SOC and enrich ^{13}C in fresh SOC and other related reactants simultaneously (Pavuluri and Kawamura 2017). While the close proximity of the $\delta^{13}C_{WSOC}$ values at urban sites (-25.77±0.04‰) to the background site (DP, -25.96‰) suggests that the WSOC in different areas of Shenzhen may share a similar origin.

https://doi.org/10.5194/egusphere-2024-736
Preprint. Discussion started: 22 March 2024

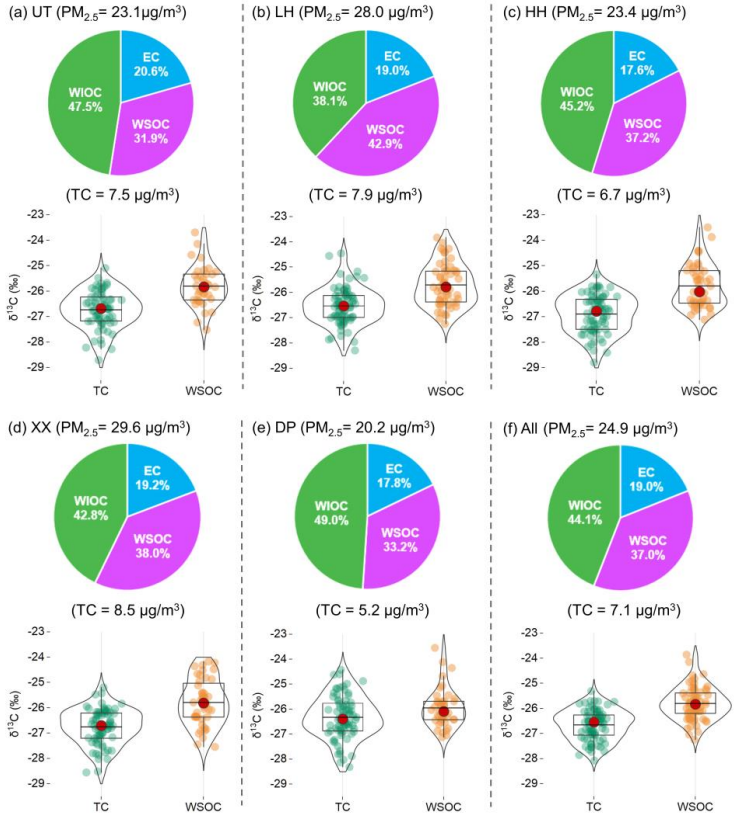

234

235 **Figure 3.** Chemical compositions of TC, $\delta^{13}C_{TC}$, and $\delta^{13}C_{WSOC}$ in $PM_{2.5}$ at urban sites (a-d), background

236 site (e), and average result from all five sites (f). The Violin Box-and-Line Plots on the right display

237 spatial variations of $\delta^{13}C_{TC}$ and $\delta^{13}C_{WSOC}$ at each site, featuring mean values (black lines) and median

238 values (red dots)

239 **3.2 Source apportionment results for TC and WSOC**

240 The BSIM model assessed the contributions of traffic source, fresh SOC, aged SOC, and biomass burning

241 (BB) to TC and WSOC, as shown in Fig. 4. On average, SOC (total of fresh and aged SOC) and traffic

242 emerged as the two major contributors to TC, accounting for 43 % and 40 % respectively, while biomass

243 burning contributed 17 % to TC. The contribution of aged SOC to TC (23 %) is comparable with fresh

https://doi.org/10.5194/egusphere-2024-736
Preprint. Discussion started: 22 March 2024

SOC (20 %). Regarding WSOC, SOC was the dominant source, comprising 45 % of aged SOC and 28 % of fresh SOC, followed by BB (18 %) and Traffic (9 %). The noteworthy contribution of aged SOC to WSOC suggests a comparatively higher water solubility of aged SOC in Shenzhen.

To evaluate the BSIM model's performance, we employed the PMF model to apportion the sources of TC and WSOC. The obtained results were subsequently compared with those from the BSIM model, as depicted in Fig. 4a. Seventeen chemical species of $PM_{2.5}$ were applied as the PMF model input to estimate source contributions to TC, encompassing carbon components, soluble inorganic ions, and elements. For the apportionment of WSOC sources, five species including WSOC, WIOC, and three organic mass spectra were applied as the PMF model input. More details about the PMF model and results can be found in the Supplementary Information (Text S1, Fig. S2-S4). PMF identified the traffic as the predominant contributor to TC (55 %), followed by SOC (34 %) and biomass burning (4 %). Concerning WSOC, aged SOC and fresh SOC were the two major sources as well, accounting for 43 % and 27 %, respectively. The traffic contribution to TC apportioned by the PMF model is higher than that of the BSIM model (55 % vs. 40 %), which may be due to the fact that some of the fresh SOC generated by the conversion of primary vehicle emissions was improperly apportioned to the traffic source in the PMF model (Li et al., 2022; Zhao et al., 2014). Previous study also showed that SOA contributes more to carbonaceous aerosols in Shenzhen than the traffic source (Cao et al., 2022). The PMF model results for WSOC were generally consistent with BSIM model results, with deviations primarily attributed to the differences in the principles and uncertainties of the two models.

Furthermore, this study examined cumulative frequency distributions to elucidate the inherent uncertainty in source apportionments of TC and WSOC. As shown in Fig. S5a and b, the proportional contributions of BB source to both TC and WSOC were quite stable during the research periods due to

https://doi.org/10.5194/egusphere-2024-736
Preprint. Discussion started: 22 March 2024

its low UI_{90} value (0.02). This may be attributed to the incorporation of mass spectral constraints for the BB source in the BSIM model used in this study. For TC source apportionment results, the largest UI_{90} value (0.46) was observed for the traffic source, indicating that its contribution to TC exhibited relatively high uncertainty. In 90 % probability, its contribution ranged from 19.4 % to 60.9 %. The UI_{90} values for fresh and aged SOC were 0.15 and 0.30, respectively. Regarding WSOC, the calculated UI_{90} value of traffic, fresh SOC, and aged SOC ranged from 0.18 to 0.24. The UI_{90} values obtained through the BSIM model remained within reasonable limits, and were smaller than those calculated in previous related studies (0.23-0.62) (Zaryab et al., 2022; Ji et al., 2017). Consequently, the source contributions of TC and WSOC estimated by the BSIM model in this study were deemed reasonable.

For seasonal variations, as shown in Fig. 4b, SOC still was the major source of TC and WSOC during all four seasons, ranging from 38 % ~ 46 % and 71 % ~ 75 % respectively. Significant high contributions of fresh SOC to TC and WSOC occurred in summer (27 %, 39 %), and relatively higher contributions of aged SOC to TC and WSOC were observed in winter (26 %, 52 %). It is because meteorological conditions in winter characterized by inversions and stagnant winds facilitate the accumulation of air pollutants, and Shenzhen is largely influenced by regional pollution transport in winter, favoring the formation of aged SOC (Huang et al., 2018). In contrast, favorable meteorological conditions (e.g. intense and prolonged solar radiation, high temperatures, and relative humidity) in summer enhanced photochemical reactions to generate fresh SOC. In terms of spatial distributions (Fig. 4c), the contributions of the traffic source to TC were higher at urban sites (38 % to 43 %) compared to the background site (34 %). This finding aligns with expectations due to increased human activity and vehicle numbers in urban locations. At the DP site, the contributions of SOC to TC were higher than those of other sources (47 %), signifying a predominant influence of regionally transported pollutant

https://doi.org/10.5194/egusphere-2024-736
Preprint. Discussion started: 22 March 2024

288 emissions on TC at the background site. However, the contributions of SOC and the other two primary
289 sources at both urban and background sites were all close to each other, indicating the source composition
290 of WSOC in Shenzhen is less affected by air pollution degree compared to TC.

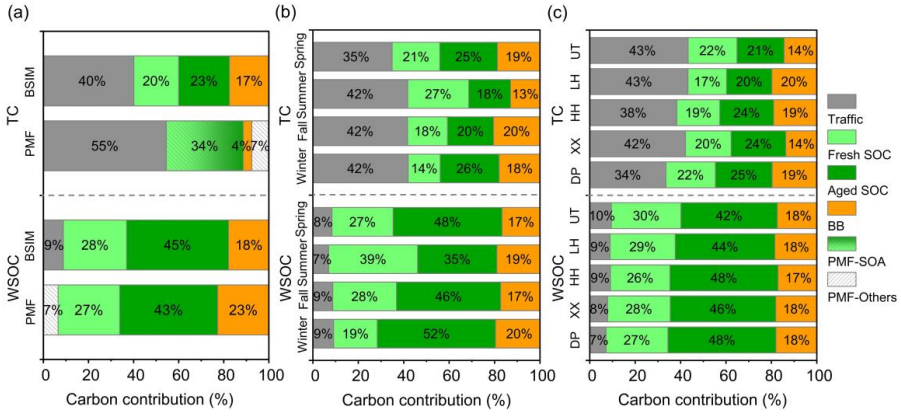

291

292 **Figure 4.** (a) Comparison of source apportionment results between BSIM model and PMF model for TC
293 and WSOC, (b) seasonal and (c) spatial distributions of source apportionment results for TC and WSOC
294 based on the BSIM model.

295 **3.3 Water solubility of fresh SOC and aged SOC**

296 The contributions of fresh SOC and aged SOC to WIOC were the differences between the contributions
297 of those two SOC sources to TC and WSOC from the BSIM model (Sect. 2.4) in this study. As shown in
298 Fig. 5a, fresh SOC and aged SOC made contributions of 23.2±4.2 % and 13.4±3.8 % to WIOC,
299 respectively, implying that primary sources are the dominant contributors to WIOC. Further support for
300 this finding is evident in the strong correlation between WIOC and EC, as depicted in Fig. 5b and c. A
301 higher WIOC/EC ratio was observed in winter (2.9) than in other seasons, consistent with the highest
302 contributions of aged SOC to WIOC in winter (22 %). This observation implies that WIOC in winter is
303 influenced not only by local primary sources but also by the promotion of secondary pollution.

https://doi.org/10.5194/egusphere-2024-736
Preprint. Discussion started: 22 March 2024

To investigate deeply the water solubility characteristics of fresh and aged SOC, we then calculate their water-soluble fraction by comparing their water-soluble portion to the ambient fraction ($[c]_{water\text{-}soluble}/([c]_{water\text{-}soluble}+[c]_{water\text{-}insoluble})$) (Li et al., 2021). As shown in Fig. 5d, the overall water-soluble fraction of SOC in this study was 66.2 % with a range from 58.9 % to 76.0 %. Fresh SOC exhibited a much lower water-solubility of 54.2 %, whereas aged SOC displayed a comparatively higher water-solubility of 76.5 %. The higher water solubility of aged SOC compared to fresh SOC might be due to the positive correlation between aerosol hygroscopicity and oxidation in the sub-saturated state. The water-soluble fraction of SOC in this study was close to that reported in other coastal cities (Tokyo (71 %) and Southeastern United States (60 %)) (Kondo et al., 2007; Verma et al., 2015), while was much higher than that reported in northern Chinese cities (Beijing (42 % ~ 45 %) and Handan (49 %)) (Li et al., 2021; Qiu et al., 2019). In addition, the water-soluble fraction of both fresh SOC and aged SOC, as calculated in this study, was comparable to that reported in Guangzhou (61 % and 86 % for fresh and aged SOC respectively) (Xiao et al., 2011). This could be attributed to Shenzhen's coastal location, which is markedly influenced by regional transport from neighboring urban areas and the eastern seaboard air masses. The high relative humidity facilitates the conversion of aged SOC into WSOC during the pollution transport process. This result is in accordance with previous findings that air masses influenced by anthropogenic emissions could promote the formation of high water-soluble SOA under high relative humidity in urban environments (Miyazaki et al., 2006; Salma et al., 2007; Weber et al., 2007). Given that the aging process of SOA dissolved in water could enhance the cloud condensation nuclei (CCN) activity of the particles (Liu and Matsui 2022), high water-soluble aged SOC in Shenzhen might have significant impacts on the activity of CCN, potentially resulting in more important indirect climate effects.

The water-soluble fraction of SOC (especially aged SOC) in Shenzhen exhibits obvious seasonal

https://doi.org/10.5194/egusphere-2024-736
Preprint. Discussion started: 22 March 2024

326 characteristics, with the highest in fall (76.0 %) and the lowest in winter (56.0 %). This phenomenon is
327 primary related to the robust atmospheric oxidizing capacity during fall in Shenzhen since the
328 atmospheric oxidants such as OH and NO_3 radicals play pivotal roles in driving the secondary generation
329 of WSOC (Wang et al., 2023). Conversely, during winter, the temperature and relative humidity are at
330 their lowest levels, and the relatively diminished atmospheric oxidizing capacity also constrains the
331 secondary generation of WSOC.

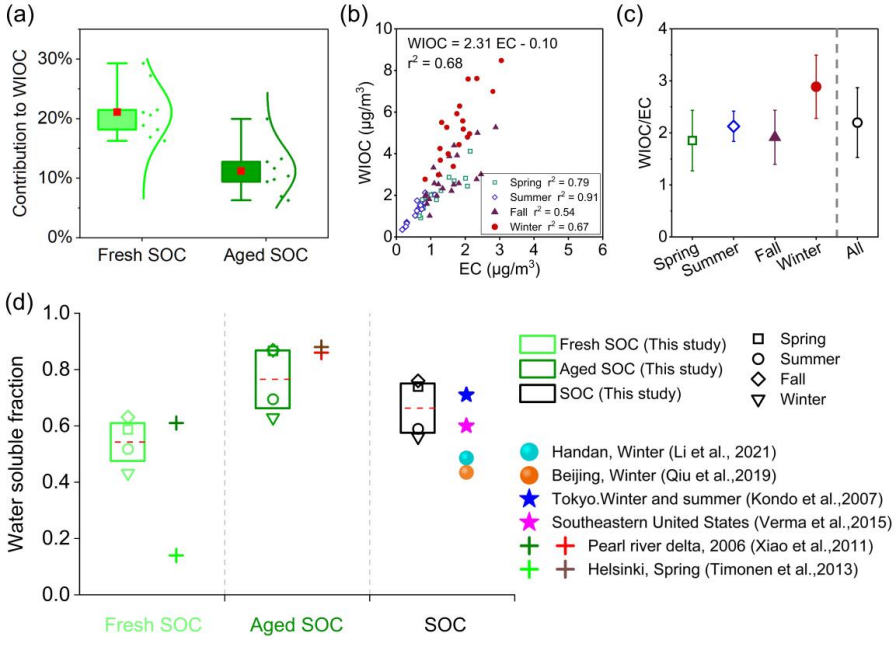

332

333 **Figure 5.** (a) Box and whisker plots of fresh and aged SOC contributions to WIOC, the upper and lower
334 of the box representing the 75th and 25th percentiles, and the red squares featuring mean values, (b)
335 Scatterplot of WIOC versus EC by season, (c) Seasonal variation of WIOC/EC ratio, (d) Comparison of
336 the water-soluble fraction of SOC (fresh SOC, aged SOC, SOC) in this study (box and whisker plots)
337 with those in other related literature (colored markings on the right). The upper and lower of the box
338 represent the 75th and 25th percentiles and the dashed red lines indicate mean values (Kondo et al., 2007;

https://doi.org/10.5194/egusphere-2024-736
Preprint. Discussion started: 22 March 2024

Li et al., 2021; Qiu et al., 2019; Timonen et al., 2013; Verma et al., 2015; Xiao et al., 2011).

4. Summary and implications

Assessing the impacts of different oxidational SOC on air quality and its water solubility has been challenging, and this work successfully evaluated the water-soluble fraction of fresh and aged SOC employing the BSIM model on one-year observational data for stable carbon isotopes and mass spectra of TC and WSOC in Shenzhen, China. Compared with other methods, e.g. PMF model, EC tracer, and multiple linear regression analyses, the BSIM model successfully calculated the contributions of fresh SOC and aged SOC to WSOC and WIOC, owing to prior and localized information about stable carbon isotopes and mass spectra of $PM_{2.5}$ sources. Therefore, establishing localized carbonaceous aerosol source profiles for stable carbon isotopes becomes crucial for comprehending the relationship between the aging degree and water solubility of SOC.

The observed average mass concentration of $PM_{2.5}$ during the sampling period in Shenzhen was 24.9 μg/m^3, and WSOC accounts for 48 % of OC. The mean stable carbon isotope values for TC ($\delta^{13}C_{TC}$) and WSOC ($\delta^{13}C_{WSOC}$) were -26.64 ± 0.79 ‰ and -25.80 ± 0.88 ‰, respectively. WSOC was dominated by secondary sources while WIOC was dominated by primary sources. The contribution of fresh SOC and aged SOC to WSOC, WIOC were 28.1 % and 45.2 %, 23.2 % and 13.4 %, respectively. The overall water-soluble fraction of SOC in this study was 66.2 %, with aged SOC constituting 76.5 % and fresh SOC 54.2 %. The water-soluble fraction of aged SOC was 22 % higher than fresh SOC, even though both of them demonstrated remarkable water-soluble characteristics in Shenzhen. This finding highlights the important role of aged SOC in the water uptake process of particulate matter. Considering the strong correlation between the water solubility of SOC and its light extinction effect, further exploration of the

https://doi.org/10.5194/egusphere-2024-736
Preprint. Discussion started: 22 March 2024

extinction effect of SOC with different aging degrees will greatly contribute to a more profound understanding of the extinction mechanism of SOC. Besides, the water solubility of SOC in coastal cities was observed to be higher than that in inland cities, suggesting a more pronounced climate effect of SOC in coastal cities. Therefore, there should be increased emphasis on enhancing the control of SOA precursors in coastal urban areas to better integrate air pollution and climate change management. This is particularly crucial given the observed rise in the proportion of SOA in particulate matter in recent years. Moreover, the results of our study further hinted that the notable water solubility of SOC, particularly aged SOC, may contribute a lot to the formation of CCN above coastal cities, which is also helpful to a better understanding of the cloud microphysical processes and the indirect climate effect of SOC in coastal urban regions.

https://doi.org/10.5194/egusphere-2024-736
Preprint. Discussion started: 22 March 2024

Data availability. Datasets are available by contacting the corresponding author, Xing Peng (pengxing@pku.edu.cn)

Author contributions. PX and HX conceptualized the study. WF, CL, TM and FN retrieved and constructed the dataset. WF and PX carried out the statistical analysis. WF prepared the first draft of the manuscript, which was commented on and revised by PX, HL, and HX. All authors reviewed and approved the final version for publication.

Competing interests. The authors declare that they have no conflict of interest.

Financial support. This research has been supported by the National Key Research and Development Program of China (2023YFC3709203) and the Science and Technology Plan of Shenzhen Municipality (JCYJ20220818100812028).

https://doi.org/10.5194/egusphere-2024-736
Preprint. Discussion started: 22 March 2024

References

Cao, L. M., Huang, X. F., Li, Y. Y., Hu, M. & He, L. Y. (2018) Volatility measurement of atmospheric submicron aerosols in an urban atmosphere in southern China. *Atmos. Chem. Phys.,* 18**,** 1729-1743.

Cao, L. M., Wei, J., He, L. Y., Zeng, H., Li, M. L., Zhu, Q., Yu, G. H. & Huang, X. F. (2022) Aqueous aging of secondary organic aerosol coating onto black carbon: Insights from simultaneous L-ToF-AMS and SP-AMS measurements at an urban site in southern China. *J. Clean. Prod.,* 330.

Ceburnis, D., Garbaras, A., Szidat, S., Rinaldi, M., Fahrni, S., Perron, N., Wacker, L., Leinert, S., Remeikis, V., Facchini, M. C., Prevot, A. S. H., Jennings, S. G., Ramonet, M. & O'Dowd, C. D. (2011) Quantification of the carbonaceous matter origin in submicron marine aerosol by ^{13}C and ^{14}C isotope analysis. *Atmos. Chem. Phys.,* 11**,** 8593-8606.

Chen, T., Liu, Y., Chu, B., Liu, C., Liu, J., Ge, Y., Ma, Q., Ma, J. & He, H. (2019) Differences of the oxidation process and secondary organic aerosol formation at low and high precursor concentrations. *J Environ Sci (China).* 79**,** 256-263.

DeCarlo, P. F., Dunlea, E. J., Kimmel, J. R., Aiken, A. C., Sueper, D., Crounse, J., Wennberg, P. O., Emmons, L., Shinozuka, Y., Clarke, A., Zhou, J., Tomlinson, J., Collins, D. R., Knapp, D., Weinheimer, A. J., Montzka, D. D., Campos, T. & Jimenez, J. L. (2008) Fast airborne aerosol size and chemistry measurements above Mexico City and Central Mexico during the MILAGRO campaign. *Atmos. Chem. Phys.,* 8**,** 4027-4048.

Ding, X., Wang, X. M., Gao, B., Fu, X. X., He, Q. F., Zhao, X. Y., Yu, J. Z. & Zheng, M. (2012) Tracer-based estimation of secondary organic carbon in the Pearl River Delta, south China. *J. Geophys. Res. Atmos.,* 117**,** 1-14.

Docherty, K. S., Stone, E. A., Ulbrich, I. M., DeCarlo, P. F., Snyder, D. C., Schauer, J. J., Peltier, R. E.,

https://doi.org/10.5194/egusphere-2024-736
Preprint. Discussion started: 22 March 2024

Weber, R. J., Murphy, S. M., Seinfeld, J. H., Grover, B. D., Eatough, D. J. & Jimenez, J. L. (2008) Apportionment of primary and secondary organic aerosols in Southern California during the 2005 study of organic aerosols in riverside (SOAR-1). *Environ. Sci. Technol.,* 42**,** 7655-7662.

Donaldson, D. J. & George, C. (2012) Sea-surface chemistry and its impact on the marine boundary layer. *Environ. Sci. Technol.,* 46**,** 10385-10389.

Favez, O., Sciare, J., Cachier, H., Alfaro, S. C. & Abdelwahab, M. M. (2008) Significant formation of water-insoluble secondary organic aerosols in semi-arid urban environment. *Geophys. Res. Lett.,* 35.

Fushimi, A., Wagai, R., Uchida, M., Hasegawa, S., Takahashi, K., Kondo, M., Hirabayashi, M., Morino, Y., Shibata, Y., Ohara, T., Kobayashi, S. & Tanabe, K. (2011) Radiocarbon (^{14}C) diurnal variations in fine particles at sites downwind from Tokyo, Japan in summer. *Environ. Sci. Technol.,* 45**,** 6784-92.

Han, S., Hong, J., Luo, Q., Xu, H., Tan, H., Wang, Q., Tao, J., Zhou, Y., Peng, L., He, Y., Shi, J., Ma, N., Cheng, Y. & Su, H. (2022) Hygroscopicity of organic compounds as a function of organic functionality, water solubility, molecular weight, and oxidation level. *Atmos. Chem. Phys.,* 22**,** 3985-4004.

He, L. Y., Lin, Y., Huang, X. F., Guo, S., Xue, L., Su, Q., Hu, M., Luan, S. J. & Zhang, Y. H. (2010) Characterization of high-resolution aerosol mass spectra of primary organic aerosol emissions from Chinese cooking and biomass burning. *Atmos. Chem. Phys.,* 10**,** 11535-11543.

Huang, R. J., Zhang, Y., Bozzetti, C., Ho, K. F., Cao, J. J., Han, Y., Daellenbach, K. R., Slowik, J. G., Platt, S. M., Canonaco, F., Zotter, P., Wolf, R., Pieber, S. M., Bruns, E. A., Crippa, M., Ciarelli, G., Piazzalunga, A., Schwikowski, M., Abbaszade, G., Schnelle-Kreis, J., Zimmermann, R., An, Z., Szidat, S., Baltensperger, U., El Haddad, I. & Prevot, A. S. (2014) High secondary aerosol contribution to particulate pollution during haze events in China. *Nature.,* 514**,** 218-22.

https://doi.org/10.5194/egusphere-2024-736
Preprint. Discussion started: 22 March 2024

427 Huang, X. F., Zou, B. B., He, L. Y., Hu, M., Prévôt, A. S. H. & Zhang, Y. H. (2018) Exploration of $PM_{2.5}$
428 sources on the regional scale in the Pearl River Delta based on ME-2 modeling. *Atmos. Chem. Phys.,*
429 18**,** 11563-11580.
430 Ji, X. L., Xie, R. T., Hao, Y. & Lu, J. (2017) Quantitative identification of nitrate pollution sources and
431 uncertainty analysis based on dual isotope approach in an agricultural watershed. *Environ. Pollut.,*
432 229**,** 586-594.
433 Jiang, F., Liu, J., Cheng, Z., Ding, P., Xu, Y., Zong, Z., Zhu, S., Zhou, S., Yan, C., Zhang, Z., Zheng, J.,
434 Tian, C., Li, J. & Zhang, G. (2022) Dual-carbon isotope constraints on source apportionment of black
435 carbon in the megacity Guangzhou of the Pearl River Delta region, China for 2018 autumn season.
436 *Environ. Pollut.,* 294**,** 118638.
437 Kaul, D. S., Gupta, T., Tripathi, S. N., Tare, V. & Collett, J. L. (2011) Secondary organic aerosol: a
438 comparison between foggy and nonfoggy days. *Environ. Sci. Technol.,* 45**,** 7307-7313.
439 Kirillova, E. N., Andersson, A., Sheesley, R. J., Kruså, M., Praveen, P. S., Budhavant, K., Safai, P. D.,
440 Rao, P. S. P. & Gustafsson, Ö. (2013) ^{13}C- and ^{14}C-based study of sources and atmospheric processing
441 of water-soluble organic carbon (WSOC) in South Asian aerosols. *J. Geophys. Res. Atmos.,* 118**,** 614-
442 626.
443 Kondo, Y., Miyazaki, Y., Takegawa, N., Miyakawa, T., Weber, R. J., Jimenez, J. L., Zhang, Q. & Worsnop,
444 D. R. (2007) Oxygenated and water-soluble organic aerosols in Tokyo. *J. Geophys. Res. Atmos.,* 112.
445 Li, H., Zhang, Q., Jiang, W., Collier, S., Sun, Y., Zhang, Q. & He, K. (2021) Characteristics and sources
446 of water-soluble organic aerosol in a heavily polluted environment in Northern China. *Sci. Total*
447 *Environ.,* 758**,** 143970.
448 Li, S. Y., Liu, D. T., Kong, S. F., Wu, Y. Z., Hu, K., Zheng, H., Cheng, Y., Zheng, S. R., Jiang, X. T., Ding,

https://doi.org/10.5194/egusphere-2024-736
Preprint. Discussion started: 22 March 2024

S., Hu, D. W., Liu, Q., Tian, P., Zhao, D. L. & Sheng, J. J. (2022) Evolution of source attributed organic aerosols and gases in a megacity of central China. *Atmos. Chem. Phys.,* 22**,** 6937-6951.

Lim, S., Hwang, J., Lee, M., Czimczik, C. I., Xu, X. & Savarino, J. (2022) Robust Evidence of ^{14}C, ^{13}C, and ^{15}N Analyses Indicating Fossil Fuel Sources for Total Carbon and Ammonium in Fine Aerosols in Seoul Megacity. *Environ. Sci. Technol.,* 56**,** 6894-6904.

Liu, L., Kuang, Y., Zhai, M., Xue, B., He, Y., Tao, J., Luo, B., Xu, W., Tao, J., Yin, C., Li, F., Xu, H., Deng, T., Deng, X., Tan, H. & Shao, M. (2022) Strong light scattering of highly oxygenated organic aerosols impacts significantly on visibility degradation. *Atmos. Chem. Phys.,* 22**,** 7713-7726.

Liu, M. X. & Matsui, H. (2022) Secondary organic aerosol formation regulates cloud condensation nuclei in the global remote troposphere. *Geophys. Res. Lett.,* 49.

Mahrt, F., Peng, L., Zaks, J., Huang, Y., Ohno, P. E., Smith, N. R., Gregson, F. K. A., Qin, Y., Faiola, C. L., Martin, S. T., Nizkorodov, S. A., Ammann, M. & Bertram, A. K. (2022) Not all types of secondary organic aerosol mix: two phases observed when mixing different secondary organic aerosol types. *Atmos. Chem. Phys.,* 22**,** 13783-13796.

Miyazaki, Y., Kondo, Y., Takegawa, N., Komazaki, Y., Fukuda, M., Kawamura, K., Mochida, M., Okuzawa, K. & Weber, R. J. (2006) Time-resolved measurements of water-soluble organic carbon in Tokyo. *J. Geophys. Res. Atmos.,* 111.

Parnell, A. C., Inger, R., Bearhop, S. & Jackson, A. L. (2010) Source partitioning using stable isotopes: coping with too much variation. *PLoS One.,* 5**,** e9672.

Parnell, A. C., Phillips, D. L., Bearhop, S., Semmens, B. X., Ward, E. J., Moore, J. W., Jackson, A. L., Grey, J., Kelly, D. J. & Inger, R. (2013) Bayesian stable isotope mixing models. *Environmetrics.,* 24**,** 387-399.

https://doi.org/10.5194/egusphere-2024-736
Preprint. Discussion started: 22 March 2024

471 Pavuluri, C. M. & Kawamura, K. (2017) Seasonal changes in TC and WSOC and their ^{13}C isotope ratios
472 in Northeast Asian aerosols: land surface-biosphere-atmosphere interactions. *Acta Geochimica,* 36**,**
473 355-358.
474 Plasencia Sánchez, E., Sánchez-Soberón, F., Rovira, J., Sierra, J., Schuhmacher, M., Soler, A., Torrentó,
475 C. & Rosell, M. (2023) Integrating dual C and N isotopic approach to elemental and mathematical
476 solutions for improving the PM source apportionment in complex urban and industrial cities: Case of
477 Tarragona - Spain. *Atmos. Environ.,* 293.
478 Presto, A., Miracolo, M., Kroll, J., Worsnop, D., Robinson, A. & Donahue, N. (2009) Intermediate-
479 volatility organic compounds: a potential source of ambient oxidized organic aerosol. *Environ. Sci.*
480 *Technol.,* 43**,** 4744–4749.
481 Pye, H. O. T., Murphy, B. N., Xu, L., Ng, N. L., Carlton, A. G., Guo, H., Weber, R., Vasilakos, P., Appel,
482 K. W., Budisulistiorini, S. H., Surratt, J. D., Nenes, A., Hu, W., Jimenez, J. L., Isaacman-VanWertz,
483 G., Misztal, P. K. & Goldstein, A. H. (2017) On the implications of aerosol liquid water and phase
484 separation for organic aerosol mass. *Atmos. Chem. Phys.,* 17**,** 343-369.
485 Qiu, Y., Xie, Q., Wang, J., Xu, W., Li, L., Wang, Q., Zhao, J., Chen, Y., Chen, Y., Wu, Y., Du, W., Zhou,
486 W., Lee, J., Zhao, C., Ge, X., Fu, P., Wang, Z., Worsnop, D. R. & Sun, Y. (2019) Vertical
487 characterization and source apportionment of water-soluble organic aerosol with high-resolution
488 aerosol mass spectrometry in Beijing, China. *ACS Earth Space Chem.,* 3**,** 273-284.
489 Salma, I., Ocskay, R., Chi, X. & Maenhaut, W. (2007) Sampling artefacts, concentration and chemical
490 composition of fine water-soluble organic carbon and humic-like substances in a continental urban
491 atmospheric environment. *Atmos. Environ.,* 41**,** 4106-4118.
492 Shen, Z., Zhang, Q., Cao, J., Zhang, L., Lei, Y., Huang, Y., Huang, R. J., Gao, J., Zhao, Z., Zhu, C., Yin,

https://doi.org/10.5194/egusphere-2024-736
Preprint. Discussion started: 22 March 2024

X., Zheng, C., Xu, H. & Liu, S. (2017) Optical properties and possible sources of brown carbon in $PM_{2.5}$ over Xi'an, China. *Atmos. Environ.,* 150**,** 322-330.

Shrivastava, M., Cappa, C. D., Fan, J. W., Goldstein, A. H., Guenther, A. B., Jimenez, J. L., Kuang, C., Laskin, A., Martin, S. T., Ng, N. L., Petaja, T., Pierce, J. R., Rasch, P. J., Roldin, P., Seinfeld, J. H., Shilling, J., Smith, J. N., Thornton, J. A., Volkamer, R., Wang, J., Worsnop, D. R., Zaveri, R. A., Zelenyuk, A. & Zhang, Q. (2017) Recent advances in understanding secondary organic aerosol: Implications for global climate forcing. *Rev. Geophys.,* 55**,** 509-559.

Tang, T., Cheng, Z., Xu, B., Zhang, B., Zhu, S., Cheng, H., Li, J., Chen, Y. & Zhang, G. (2020) Triple Isotopes $\delta^{13}C$, $\delta^{2}H$, and $\delta^{14}C$ Compositions and Source Apportionment of Atmospheric Naphthalene: A Key Surrogate of Intermediate-Volatility Organic Compounds (IVOCs). *Environ. Sci. Technol.,* 54**,** 5409-5418.

Timonen, H., Carbone, S., Aurela, M., Saarnio, K., Saarikoski, S., Ng, N. L., Canagaratna, M. R., Kulmala, M., Kerminen, V.-M., Worsnop, D. R. & Hillamo, R. (2013) Characteristics, sources and water-solubility of ambient submicron organic aerosol in springtime in Helsinki, Finland. *J Aerosol Sci.,* 56**,** 61-77.

Verma, V., Fang, T., Xu, L., Peltier, R. E., Russell, A. G., Ng, N. L. & Weber, R. J. (2015) Organic aerosols associated with the generation of reactive oxygen species (ROS) by water-soluble $PM_{2.5}$. *Environ. Sci. Technol.,* 49**,** 4646-56.

Vodicka, P., Kawamura, K., Schwarz, J. & Zdimal, V. (2022) Seasonal changes in stable carbon isotopic composition in the bulk aerosol and gas phases at a suburban site in Prague. *Sci. Total Environ.,* 803**,** 149767.

Wang, Y., Feng, Z., Yuan, Q., Shang, D., Fang, Y., Guo, S., Wu, Z., Zhang, C., Gao, Y., Yao, X., Gao, H.

https://doi.org/10.5194/egusphere-2024-736
Preprint. Discussion started: 22 March 2024

515 & Hu, M. (2023) Environmental factors driving the formation of water-soluble organic aerosols: A
516 comparative study under contrasting atmospheric conditions. *Sci. Total Environ.,* 866**,** 161364.
517 Weber, R. J., Sullivan, A. P., Peltier, R. E., Russell, A., Yan, B., Zheng, M., de Gouw, J., Warneke, C.,
518 Brock, C., Holloway, J. S., Atlas, E. L. & Edgerton, E. (2007) A study of secondary organic aerosol
519 formation in the anthropogenic-influenced southeastern United States. *J. Geophys. Res. Atmos.,* 112.
520 Widory, D., Roy, S., Le Moullec, Y., Goupil, G., Cocherie, A. & Guerrot, C. (2004) The origin of
521 atmospheric particles in Paris: a view through carbon and lead isotopes. *Atmos. Environ.,* 38**,** 953-
522 961.
523 Wong, J. P., Zhou, S. & Abbatt, J. P. (2015) Changes in secondary organic aerosol composition and mass
524 due to photolysis: relative humidity dependence. *J. Phys. Chem. A.,* 119**,** 4309-16.
525 Wu, Y., Huang, X., Jiang, Z., Liu, S. & Cui, L. (2020) Composition and sources of aerosol organic matter
526 in a highly anthropogenic influenced semi-enclosed bay: Insights from excitation-emission matrix
527 spectroscopy and isotopic evidence. *Atmos Res.,* 241.
528 Xiao, H. W., Xu, Y. & Xiao, H. Y. (2023) Source apportionment of black carbon aerosols in winter across
529 China. *Atmos. Environ.,* 298.
530 Xiao, R., Takegawa, N., Zheng, M., Kondo, Y., Miyazaki, Y., Miyakawa, T., Hu, M., Shao, M., Zeng, L.,
531 Gong, Y., Lu, K., Deng, Z., Zhao, Y. & Zhang, Y. H. (2011) Characterization and source
532 apportionment of submicron aerosol with aerosol mass spectrometer during the PRIDE-PRD 2006
533 campaign. *Atmos. Chem. Phys.,* 11**,** 6911-6929.
534 Yao, P., Huang, R. J., Ni, H. Y., Kairys, N., Yang, L., Meijer, H. A. J. & Dusek, U. (2022) ^{13}C signatures
535 of aerosol organic and elemental carbon from major combustion sources in China compared to
536 worldwide estimates. *Sci. Total Environ.,* 810.

https://doi.org/10.5194/egusphere-2024-736
Preprint. Discussion started: 22 March 2024

537 Zaryab, A., Nassery, H. R., Knoeller, K., Alijani, F. & Minet, E. (2022) Determining nitrate pollution
538 sources in the Kabul Plain aquifer (Afghanistan) using stable isotopes and Bayesian stable isotope
539 mixing model. *Sci. Total Environ.,* 823.
540 Zhang, Y. L., Li, J., Zhang, G., Zotter, P., Huang, R. J., Tang, J. H., Wacker, L., Prevot, A. S. & Szidat, S.
541 (2014) Radiocarbon-based source apportionment of carbonaceous aerosols at a regional background
542 site on Hainan Island, South China. *Environ. Sci. Technol.,* 48**,** 2651-9.
543 Zhao, Y. L., Hennigan, C. J., May, A. A., Tkacik, D. S., de Gouw, J. A., Gilman, J. B., Kuster, W. C.,
544 Borbon, A. & Robinson, A. L. (2014) Intermediate-volatility organic compounds: a large source of
545 secondary organic aerosol. *Environ. Sci. Technol.,* 48**,** 13743-13750.
546 Zhu, Q., He, L. Y., Huang, X. F., Cao, L. M., Gong, Z. H., Wang, C., Zhuang, X. & Hu, M. (2016)
547 Atmospheric aerosol compositions and sources at two national background sites in northern and
548 southern China. *Atmos. Chem. Phys.,* 16**,** 10283-10297.

549